

with small ellipticity and slight anisotropy. The dashed line shows the trajectory followed by $[v_o(i)/\sigma_o, \epsilon_{app}(i)]$ when i decreases from 90° (equator on) while ϵ_{true} , the true ellipticity, and δ , the anisotropy parameter, are held constant. For both of these clusters results are given for $i = 90^\circ$ and 60° .

Masses and Mass-Luminosity Ratios

The simultaneous knowledge of the velocity dispersion $\sigma(r) = \sqrt{v^2(r)}$ (corrected for rotation) and of the normalized space density distribution $v(r) = \varrho(r)/\varrho(0)$ of a population of test particles (here the giant star population) moving in a spherical cluster allows, under the hypothesis of the velocity dispersion isotropy, to determine directly the total gravitational potential. In the same order of approximation, the weak rotation can here be neglected. It is then possible to deduce the total dynamical mass $M(r)$ inside the radius r of the cluster, via the following equation:

$$\frac{GM(r)}{r} = -\sigma^2 \left[\frac{d \ln v}{d \ln r} + \frac{d \ln \sigma^2}{d \ln r} + 2\beta \right]$$

where $\beta = 0$ for the systems with isotropic velocity dispersion. However, in globular cluster cores, the limited number of stars for which the radial velocity can be determined does not allow a sufficiently precise determination of $\sigma(r)$ in order to give the variations of $d \ln \sigma^2 / d \ln r$ in the central regions. The same lack of accuracy affects the knowledge of $d \ln v / d \ln r$.

If we suppose on the one hand that the cluster consists of several sub-populations with different individual masses and, on the other hand, equipartition of the energy, the shape of the function $\sigma(r)$ can be deduced. The radial variation of $\sigma(r)$ depends on the percentage of heavy remnants (degenerated stars with masses larger than the mass of the test particles), on the mass function of the main sequence and on the total mass of the cluster. Certainly, such an approach would benefit from

a better defined luminosity function of the lower part of the main sequence (an expected task for the Space Telescope).

The observed dependence of the velocity dispersion with the distance to the centre implies, for any chosen IMF compatible with the total luminosity constraint, the presence of heavy remnants in the core of ω Cen. These objects, with individual masses larger than the giant stars by a factor of 2 or 3, represent about 7 per cent of the total mass of the cluster. Due to mass segregation, the ratio of the density of heavy remnants to the total density is very large in the nucleus (for ω Cen this ratio can be of about 35 %).

On the other hand, the radial velocity dispersion of 47 Tuc seems to require only 1 to 3 per cent of heavy remnants in comparison to the total mass.

For these two globular clusters, the total masses derived from our analysis are:

$$\begin{aligned} \text{total mass of } \omega \text{ Cen} &\approx 2.9 \cdot 10^6 \text{ solar masses} \\ \text{total mass of 47 Tuc} &\approx 1.3 \cdot 10^6 \text{ solar masses} \end{aligned}$$

which implies mass-to-luminosity ratios between 2 and 3.

The sub-population with individual masses between 1.5 and 2 solar masses consists most probably of the remnants issued from the evolution of the most massive stars of the globular clusters initial mass function. But part of this sub-population could also be binaries. The observed radial distribution of X-ray sources in globular clusters presents a notable concentration towards the core, in agreement with the dynamical segregation of individual masses of about 1.5 solar masses.

If the fact that the high stellar densities expected in collapsed cores are favourable to binary formation and if the detected X-ray sources are binaries, it would be important to recall the total absence (or at least large deficiency) of spectroscopic binaries in globular clusters. Continuing observations of stellar radial velocities, particularly in the cores of globular clusters, should create some new constraints regarding their dynamics.

R136a and the Central Object in the Giant HII Region NGC 3603 Resolved by Holographic Speckle Interferometry

G. Weigelt, G. Baier and R. Ladebeck, *Physikalisches Institut Erlangen*

R136 (HD 38268) is the mysterious central object of the 30 Doradus nebula in the Large Magellanic Cloud (Walborn, 1973). R136 consists of the bright component R136a and the fainter components R136b and R136c (Feitzinger et al., 1980). There exist mainly two opinions about the nature of R136a: that it is either a supermassive object with $M \sim 1,000$ to $3,000 M_\odot$ (Schmidt-Kaler and Feitzinger, 1981; Cassinelli et al., 1981) or that it is a dense star cluster consisting of O and WR stars (Moffat and Seggewiss, 1983; Melnick, 1983).

Speckle interferometry observations (Labeyrie, 1970) of R136a have been reported by Weigelt (1981), Meaburn et al. (1982) and Weigelt (1984). Our speckle measurements of the $0''.5$ component are in agreement with visual observations made by Innes (1927) and Worley (1984) as well as with photographic measurements by Chu et al. (1984) and by Walker and O'Donoghue (1985).

In this paper we show the first diffraction-limited true image of R136a (Fig. 2). This image shows that R136a is a dense star cluster consisting of at least 8 stars. It was possible to reconstruct a true image of R136a1 to a8 by using R136b (separation $\sim 2''.1$) and R136c (separation $\sim 3''.3$) as deconvolution keys (holographic speckle interferometry). The

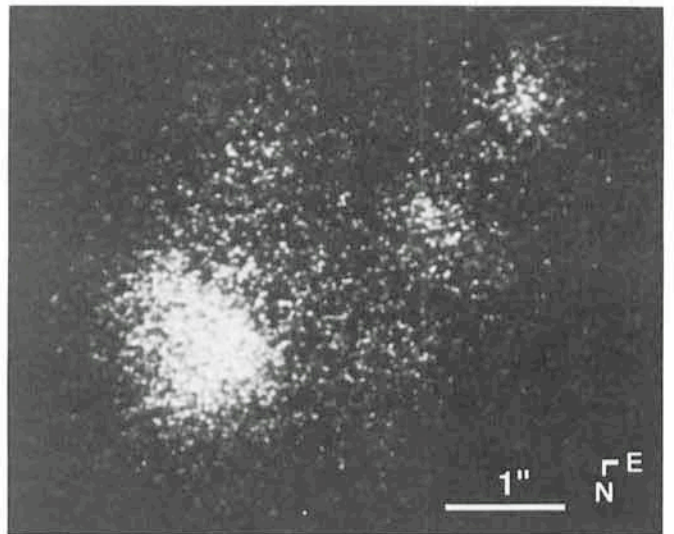


Fig. 1: Speckle interferogram of R136. The brightest speckle cloud is R136a, the other speckle clouds are R136b to e (filter RG 610, exposure time 1/15 sec).

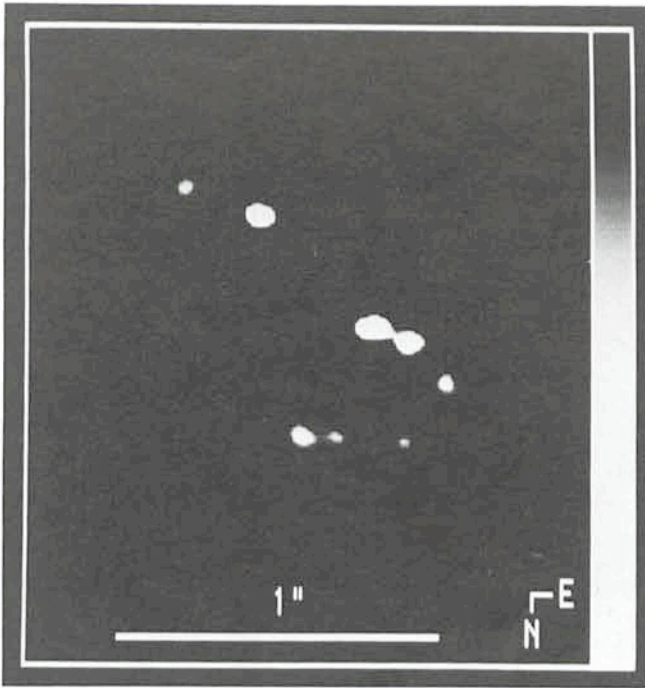


Fig. 2: Diffraction-limited image of R136 a1 to a8 reconstructed from 4,000 speckle interferograms (Danish 1.5 m telescope, filter RG 610). The dominating stars are R136 a1, R136 a2 (separation = $0''.10$) and R136 a3 (separation = $0''.48$). The double star R136 a1-a2 is the close eastern double object. The four fainter objects are R136 a4 to a8.

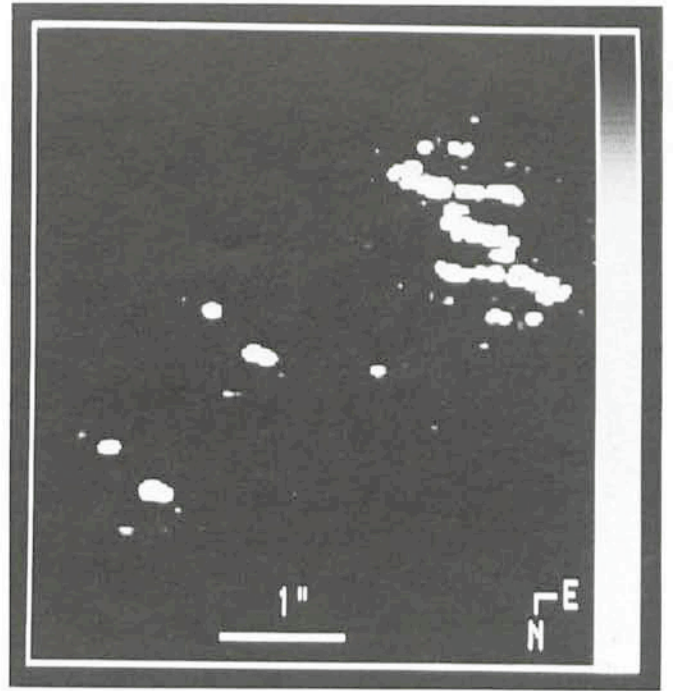


Fig. 4: One half of the autocorrelation of R136abc. It can easily be seen that the autocorrelation contains two true images of R136a caused by the holographic reference stars R136b and R136c.

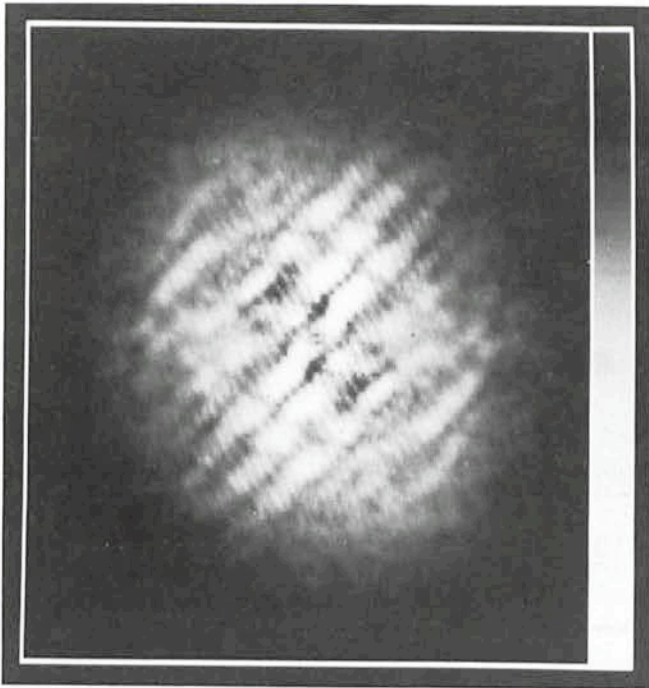


Fig. 3: Power spectrum of R136abc (= hologram of R136a).

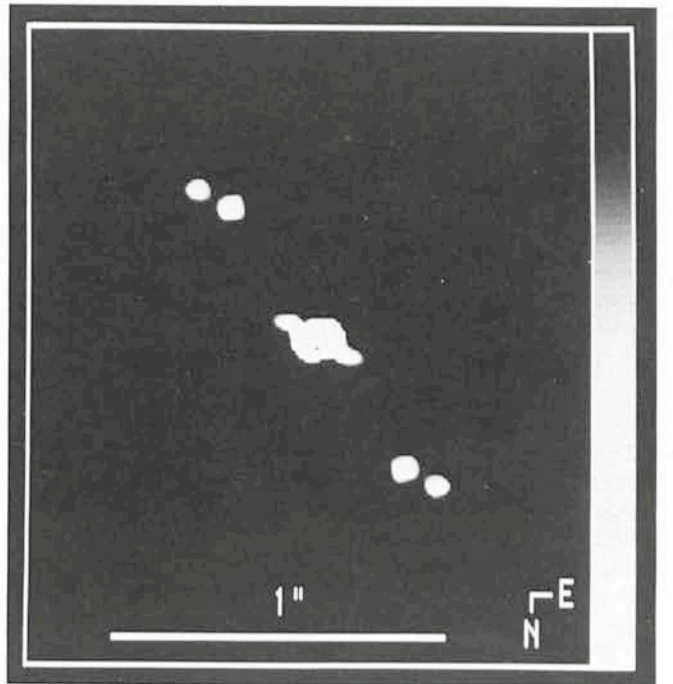


Fig. 5: Autocorrelation of R136 a1-a2-a3 reconstructed from data recorded with the 2.2 m telescope (filter $\lambda_0 = 610 \text{ nm} / \Delta\lambda = 120 \text{ nm}$). The off-axis double dot is a true image of R136a1-a2 (separation = $0''.10$).

dominating objects in R136a are the three bright stars R136 a1, a2 and a3 which have almost identical magnitudes. The separations of a1-a2 and a1-a3 are $0''.10$ and $0''.48$, respectively. The reconstructed image has a resolution of $0''.09$.

Figs. 1 to 5 show some of our speckle results. Fig. 1 is one of the speckle interferograms of R136abc recorded with the Danish 1.5 m telescope (Schott filter RG 610, S20-cathode with extended red response, exposure time 1/15 sec).

Fig. 2 is the high-resolution image of R136 a1 to a8 reconstructed digitally from 4,000 speckle interferograms (Danish 1.5 m telescope, filter RG 610).

Fig. 3 is the object power spectrum of R136abc or the hologram of R136 a1 to a8.

Fig. 4 shows one half of the autocorrelation of R136abc. The autocorrelation contains two true images of R136a which are caused by the reference stars R136b and R136c. The useful-

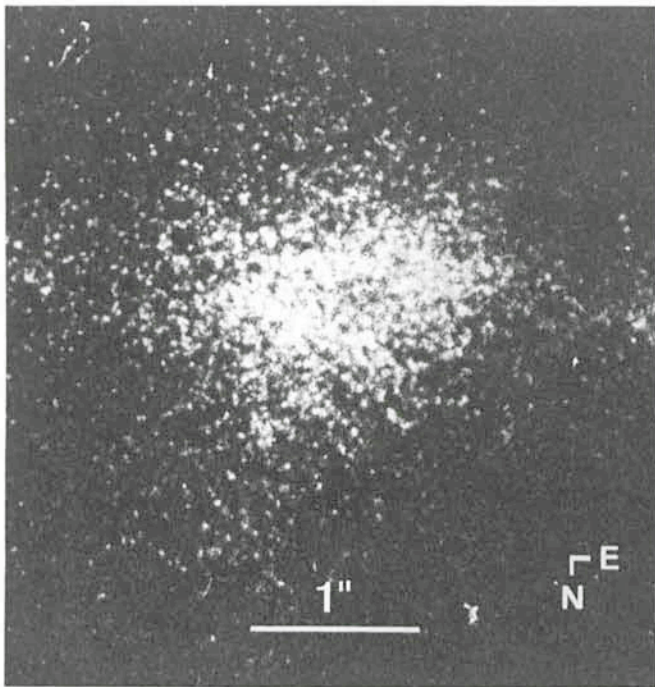


Fig. 6: Speckle interferogram of HD 97950 AB.

ness of such reference stars has been discussed by Liu and Lohmann (1973) and Weigelt (1978) in more detail.

Fig. 5 shows the autocorrelation of R136 a1–a2–a3 reconstructed from 4,000 speckle interferograms recorded with the 2.2 m telescope (filter $\lambda_0 = 610 \text{ nm}/\Delta\lambda = 120 \text{ nm}$). This autocorrelation has higher resolution than the 1.5 m autocorrelation. Therefore the a1–a2 image (= off-axis double peak) is better resolved. More details about our R136a observations are described in a paper submitted to *Astronomy and Astrophysics* (Weigelt and Baier, 1985).

Figs. 6 and 7 show one speckle interferogram and the high-resolution autocorrelation of HD 97950 AB in the giant HII region NGC 3603. We have investigated this object since it has been discussed in various papers that it may be of similar nature as R136a (Moffat and Seggewiss, 1984). The autocorrelation shows that HD 97950 AB is a star cluster consisting of 4 stars. We found that the component A is a triple star and B is a single star (see Baier et al., 1985 for more details). Since B is a single star, the three peaks on the extreme left of the autocorrelation are a true image of HD 97950 A1–A2–A3.

References

- Baier, G., Ladebeck, R., Weigelt, G.: 1985, Speckle interferometry of the central object in the giant HII region NGC 3603, submitted to *Astron. Astrophys.*
- Cassinelli, J.P., Mathis, J.C., Savage, B.D.: 1981, *Science* **212**, 1497.
- Chu, Y.-H., Cassinelli, J.P., Wolfire, M.G.: 1984, *Astrophys. J.*, **283**, 560.
- Feitzinger, J.V., Schlosser, W., Schmidt-Kaler, Th., Winkler, Chr.: 1980, *Astron. Astrophys.* **84**, 50.
- Innes, R.T.A.: 1927, Southern double star catalog, Unions Obs., Johannesburg.
- Labeyrie, A.: 1970, *Astron. Astrophys.* **6**, 85.
- Liu, C.Y.C., Lohmann, A.W.: 1973, *Optics Commun.* **8**, 372.
- Meaburn, J., Hebden, J.C., Mogan, B.L., Vine, H.: 1982, *Mon. Not. R. Astron. Soc.* **200**, 1 p.
- Melnick, J.: 1983, *The Messenger* **32**, 11.
- Moffat, A.F.J., Seggewiss, W.: 1983, *Astron. Astrophys.* **125**, 83.
- Schmidt-Kaler, Th., Feitzinger, J.V.: 1981, in: *The Most Massive Stars*, Proc. ESO workshop, eds. S. D'Odorico, D. Baade and K. Kjär, Garching, Europ. Southern Obs., p. 105.
- Walborn, N.R.: 1973, *Astrophys. J.* **182**, L21.

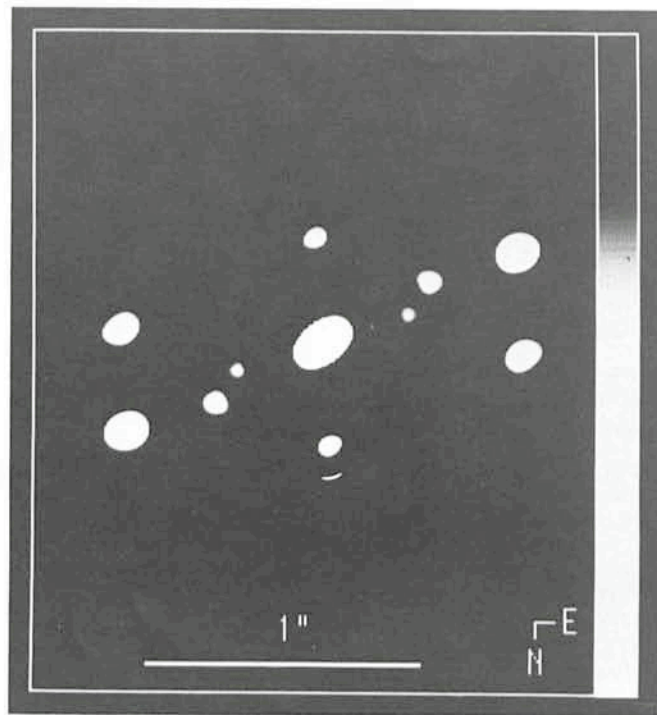


Fig. 7: High-resolution autocorrelation of HD 97950 A1–A2–A3–B. The three dots on the extreme left are a diffraction-limited image of HD 97950 A1–A2–A3.

- Walker, A.R., O'Donoghue, D.E.: R136: Multiple or Monster? in press.
- Weigelt, G.: 1978, *Appl. Opt.* **17**, 2660.
- Weigelt, G.: 1981, in Proc. of the ESO Conf. on "Scientific Importance of High Angular Resolution at IR and Optical Wavelengths", eds. M.H. Ulrich and K. Kjär, Garching, March 1981, p. 95.
- Weigelt, G.: 1984, in Proc. of the IAU Colloquium No. 79: "Very Large Telescopes, their Instrumentation and Programs, April 9–12, ESO, Garching, p. 337.
- Weigelt, G., Baier, G.: 1985, R136a in the 30 Dor nebula resolved by holographic speckle interferometry, submitted to *Astron. Astrophys.*
- Worley, C.E.: 1984, *Astrophys. J.* **278**, L109.

Access to IRAS Data in ESO Member Countries

Several of the official IRAS products have now been released to the general astronomical community, others will follow in the near future.

Already released are:

- Point Source Catalog, containing 250,000 point sources detected in at least one of the IRAS bands (12, 25, 60 and 100 μ). Print, microfiche and tape versions (2 tapes, 1,600 BPI).
- Working Survey Data Base, containing the observation history of objects in the point source catalog. Print and tape versions (2 tapes, 6,250 BPI).
- Skyflux Maps, in $16^\circ \times 16^\circ$ overlapping fields in each of the IRAS bands. These maps are preliminary, as they are based only on the third and last IRAS sky coverage (HCON3). Photographic and tape versions (188 images and 20 tapes, 6,250 BPI).
- Catalog of Low Resolution ($\lambda/\Delta\lambda = 20$) Spectra of $\approx 5,000$ sources (LRS Catalog), mainly late-type stars. Tape versions only; print version will appear in *A & A Supplements* in 1985 (1 tape, 1,600 BPI). Soon to be released will be:
- Catalog of variable sources.
- Skyflux maps containing data from all IRAS sky coverages (HCON's 1, 2 and 3 [revised]).